



Experimental Study and Numerical Modeling of Downward Flame Spread Along a Single Pine Needle: Part 1 (Experiments)

O. P. Korobeinichev^a, A. G. Shmakov^a, K. N. Osipova^a, Amit Kumar^b,
and Naresh Kambam Meetei^b

^aVoevodsky Institute of Chemical Kinetics and Combustion SB RAS, Novosibirsk, Russia; ^bDepartment of Aerospace Engineering, National Centre for Combustion Research and Development, IIT Madras, Tamil Nadu, India

ABSTRACT

This work presents an experimental study of downward flame spread over a vertically positioned single pine needle of *Pinus Sibirica*. Detailed spatial measurements in the gas phase have been carried out to determine the chemical and thermal flame structure of the spreading flame. In addition, temperature distribution in pine needle is also measured. In the gas phase micro thermocouple measurements were used to determine temperature distribution; mass spectrometry with microprobe sampling was used to measure the concentration profiles of O₂ and the main combustion products (CO₂, CO, H₂O). The micro thermocouple method was also used to measure temperature distribution in a pine needle for flame spread along it. The data obtained from the experiments on single vertical pine needles reveals two stages in downward flame propagation: (1) a zone in the vicinity of the leading edge of the spreading flame where virgin pine needle decomposes to form char and volatile pyrolysis products formed. The pyrolysis products mix with air and ignited by flame behind causes flame to propagate; and (2) a zone where heterogeneous burning of char occurs. The downward flame spread velocity along a single pine needle was also measured for several counter-flow air velocities to obtain dependence of flame spread rate on counter-flow velocity. The data obtained in this work can also serve as a much needed base for testing and refining the numerical models describing flame spread along individual components of forest fuels (FF). Further, as the flame propagation along a bed of FF is similar to that along charring polymer materials, the data obtained and the applied methods of research may be also of interest to those studying the charring polymer combustion mechanism.

ARTICLE HISTORY

Received 18 May 2017
Revised 11 September 2017
Accepted 12 September 2017

KEYWORDS

Char; flame spread velocity; flame structure; forest fuels; micro thermocouple; pine needle; pneumatic probe; probe mass spectrometry; volatile pyrolysis products

Introduction

A large number of researches (Fernandez-Pello and Williams, 1975; Hsu and T'ien, 2011; Sibulkin et al., 1974; Sirignano, 1972; Wichman, 1992) over the years have been dedicated to experimental and theoretical studies of flame spread along solid materials in a flow of oxidizing gas. An important aspect of this issue is the direction of flame spread and gas flows. These studies are of essential interest both for the fundamental and applied science, due to importance of fire

CONTACT Amit Kumar  amitk@ae.iitm.ac.in  Department of Aerospace Engineering, Indian Institute of Technology Madras, Chennai, Tamil Nadu 600036, India.

Supplemental data for this article can be accessed on the [publisher's website](#).

Color versions of one or more of the figures in the article can be found online at www.tandfonline.com/gcst.

© 2017 Taylor & Francis

safety of materials. Examples of such materials are polymers and cellulose-based materials (cardboard, paper, and wood). Components of forest fuels (FF), such as needles of pine and fir, leaves, branches, twigs, and grass, are also objects of investigations. These forest fuels together may form combustible litter, which is the source of ground forest fires.

The study of thermal and chemical processes occurring at flame spread along typical fire conductors, such as forest leaf bed, pine needles litter, grass, moss, and lichens, is of interest in terms of understanding the combustion processes and predicting the propagation of forest and steppe fires. In the regions of Siberia and the Russian Far East, prevailing are the boreal forests, in which the Siberian pine is predominant. Combustion and flame spread across pine needles litter is the main cause of catastrophic fires resulting in severe human and material losses. In this regard, an essential task is to clarify the mechanism of flame spread across pine needles litter in order to develop a model that could predict the main characteristics of a fire—the rate and direction of flame spread, the probability of buildings' ignition, fire spread across fire protection belts, etc., depending on the characteristics of the forest fuel (the type of the forest fuel, its moisture content, availability of the forest fuel per unit area, etc.), as well as on the weather conditions (the air temperature and moisture content, the wind velocity).

Over a long time, active studies have been conducted globally devoted to natural fire spread; however, many issues still remain unsolved. This is related to both a great variety and the complex composition of the forest fuels themselves and a broad range of external conditions in which their combustion is investigated. One of the approaches existing now is the study of combustion of individual components of forest and steppe fuels, followed by development of a model describing this process under different conditions. Such models are simple enough to be compared to the experimental data, as they describe combustion of a single component of the fuel, not the assemblage of components, thus there is no necessity in describing complex physical processes, such as turbulence. Later such simple models of individual types of fuels may be united into a more complex model to describe the characteristics of real fires.

In the literature on flame spread over forest fuels, the majority of the publications are devoted to the study of flame spread across a bed of different forest or steppe fuels (Albini, 1981; Konev and Sukhinin, 1977; Morandini et al., 2005; Morvan, 2013; Santoni et al., 2002; Weber, 1990). Considerably less papers are investigating the flame characteristics of individual components of these fuels, which is often caused by serious experimental challenges (Konev, 1977; Lyons and Weber, 1993; Sukhinin, 1975; Weber and De Mestre, 1990). Therefore, such studies require development of special approaches and methods, as the objects under study have small characteristic dimensions.

In the works by Sukhinin (1975) and Konev and Sukhinin (1977) thermocouples were used to measure temperature distribution in condensed and gas phases when fire was spread across a bed of shed pine needles. Several thermocouples were positioned both inside a bed of pine needles and over it. In addition, one of the thermocouples was embedded inside a pine needle. For this purpose, an opening was made in a pine needle perpendicular to its axis with a diameter of 100 microns, into which a chromel-aluminum thermocouple 50 microns in diameter was inserted, with the pine needle slightly pressed around it to ensure better contact with the thermocouple. It is noted that the variant of thermocouple positioning used in these works may result in the errors in temperature measurements, as due to the significant temperature gradient in the direction

perpendicular to the pine needle's surface, a flow of heat along the thermocouple's leads is possible causing higher temperature measurement values compared to the true temperature values inside the pine needle. In the above studies, the share of radiation in the heat balance was evaluated for flame distribution across a bed of pine needles both in the zone of convective heating and at a large distance from the flame front. The authors showed that heat exchange due to radiation did not determine the process of flame spread under the conditions studied.

In the papers by Weber and De Mestre (1990) and Lyons and Weber (1993), the influence of the angle of slope of a single pine needle on the flame spread velocity along it was investigated. Changing the angle from -90° (the flame spreads downward) to 90° (the flame spreads upward) results in the change of the flame spread velocity from 2 mm/s to 16 mm/s, eight times. In addition, the influence of a concurrent air flow velocity on the velocity of movement of a horizontally positioned pine needle was studied in this work. Experiments showed that, as the concurrent air flow velocity increases from 0 to 2 m/s, the flame spread velocity increases from 3 mm/s to 25 mm/s, nearly by an order of magnitude. The influence of the concurrent air flow velocity on the flame spread velocity along a single pine needle has not been investigated in the literature. Yet, such data may be required to evaluate the conditions under which flame distribution across a bed of pine needles becomes impossible, i.e., when it is necessary to determine the limits of fire existence.

Much of the modeling work on the flame spread (Bhattacharjee and Altenkirch, 1992; Kumar and Kumar, 2012, 2017) study relies on global data, such as flame spread rate, approximate temperature in the flame, flame shape and size obtained from the experiments. For development of more detailed models, detailed experimental data is required for checking validity of various sub models. Such experimental data has been shown to be very useful for the modeling studies (Singh and Gollner, 2015). Therefore, the purpose of this study was an experimental investigation of the thermal and chemical flame structure of a single pine needle, including measuring temperature distribution in the condensed phase, as well as determining the influence of the counter-flow air velocity on the flame spread velocity along a single pine needle. Such experimental data are required for developing and testing numerical models describing combustion of individual components of forest and steppe fuels under conditions of fire spread. As the flame propagation along a bed of FF is similar to that along polymer materials, the data obtained and the applied methods of research may also be of interest to those studying the polymer combustion mechanism.

Experiments

Fuel material

The fuel studied in this work was litter of pine needles of *Pinus Sibirica*. Straight pine needles nearly identical in size with the cross section of about $0.6 \text{ mm} \times 1.0 \text{ mm}$ and length of about 50–60 mm were selected. For the experiments, 20-mm-long specimens were cut out from the middle part of each pine needle. It was made sure that the selected pine needles were free of any visible signs of damage and resin traces. The pine needles were dried at the temperature of 60°C for a period of 24 h. This ensured that the moisture content in the same was between 7.8–9.4%. The fuel specimen was taken out of a drier

immediately before the experiment. The elementary composition of the pine needle was determined to be: C—51.78%, H—6.96%, N—1.78%, O—34.5%. The BET method (Brunauer et al., 1938) was used to determine the specific surface area, which was found to be $0.18 \text{ m}^2/\text{g}$. The specific fuel density was $600 \text{ kg}/\text{m}^3$ and the surface-to-volume ratio was 4550 m^{-1} . The measured thermal diffusivity of a pine needle was found to be $1.26 \times 10^{-6} \text{ m}^2/\text{s}$. The pyrolysis kinetics of pine needles have been studied by Korobeinichev et al. (2014).

Measuring the chemical structure of downward spreading flame over a single pine needle

Species concentration profiles in the downward spreading flame under study were measured using the method of probe mass spectrometry. A quartz tube was used as a micro probe. The probe had an internal diameter of 4 mm, external diameter of 6 mm, and length of 120 mm. One end of the probe, which was tapered, had an orifice inside the cone. The length of the conical part was 12 mm, the orifice diameter was 0.06 mm, and the thickness of the walls near the orifice was 0.06 mm. The external angle of the conic part was about 20° . A flexible vacuum tube was used to connect the above micro probe with a system of sample supply to the ion source of the quadrupole mass spectrometer (Hiden HPR-60). The pressure in the sample delivery line was about 400 Pa. The three-stage system of vacuum evacuation of this mass spectrometer was essentially modernized: at the first stage of the evacuation system, a turbo-molecular pump (VMN-500) with the performance of 500 l/s was installed instead of a fore-pump, which ensured pressure at the first stage to be at the level of 0.27 Pa. The pressure at the second stage of pumping was about $6.6 \times 10^{-3} \text{ Pa}$. At the third stage (ion source chamber of the mass spectrometer), a nitrogen trap was installed, which allowed the pressure in this part of the pumping system to be reduced to 10^{-5} Pa and, therefore, the peak intensity of the background mass spectrum to be considerably decreased.

To probe the downward spreading flame of the pine needle, a micro probe was mounted on a three-coordinate traverse mechanism, which allowed the probe to be positioned with an accuracy reaching 0.1 mm in relation to the securely fixated pine needle. The micro probe was positioned in the direction perpendicular to the pine needle's axis at the distance, which could be varied from 1 mm to 7 mm from its middle. The pine needle was fastened vertically either with a clip (secured to the lower end of the pine needle) or to the leads of the thermocouple drawn through the pine needle. The pine needle was ignited from its upper end with a miniature cotton torch wetted with ethanol, which was quickly removed after the pine needle started to burn.

To synchronize the results of measuring the composition of the combustion products with the video recording and the temperature measurements, a light-emitting diode was used, connected to a power supply with a switch. During the experiment, the operator switched the light-emitting diode on and off, with the diode leads simultaneously connected with the AD converters of the mass spectrometer and of the temperature measurement device. Thus, the glow of the diode and the image of the burning pine needle were recorded in the video and in the additional measurement channels of the mass spectrometer and of the temperature measurement device.

The error of measuring species concentrations in the flame was determined by a number of factors, among which the major ones were the errors in measuring mass peak intensities and inaccuracy in measuring the calibrating gas mixtures. The error of measuring the mass peak intensity depends on the concentration of the respective component in flame and the intensity of the peak signal in the background mass spectrum. The relative accuracy error of measuring the concentration of the main gas components was evaluated to be about ± 5 –10%.

The calibrations based on a gas mixture of known composition have shown that the background mass spectrum does not depend on the pressure at the first and second stages of mass spectrometric pumping. This allowed to determine changes in the partial pressure of the measured species in the sample by changes in the mass peak intensities of these species. The molar concentrations of the components were calculated from the values of partial pressures. In addition, supposing that the average molecular weight of the components in different flame zones varies only slightly, it is possible to determine the temperature of the gas sampled with the micro probe by that known from literature dependence of gas consumption through the probe orifice.

Table 1 shows the species and mass peaks by which concentration of these species was measured in the pine needle's flame, as well as the relative measurement errors. Concentration of O_2 , CO, and CO_2 was measured by the peak intensities of the parent masses (m/e 32, 28, 44, accordingly), concentration of N_2 was determined by the peak intensity of the fragment ion m/e 14, while that of C_2H_5OH and CH_3OCH_3 was found by the most intense peaks of the fragment ions (m/e 31 and m/e 43, accordingly). When concentration of CO was calculated, contribution to the peak of mass 28 from N_2 was taken into consideration and was determined in the calibration tests. As can be seen, the errors in the concentration measurements are essentially present; therefore, in calculating the species concentration profiles, data smoothing was used. In the given tests, the intensities of the selected mass peaks were measured six times per second, i.e., the time of measuring the concentration of one point in flame was ~ 0.17 s. With the typical downward flame spread velocity over a vertical pine needle of about 2 mm/s, spatial resolution was approximately 0.3 mm, which is close to the characteristic size of the zone of gas-dynamic perturbations of about 0.2 mm caused by the suction of gas through the probe orifice 0.06 mm in diameter. The measurements we have conducted have shown that the volume flow rate through a microprobe with the orifice diameter of 0.06 mm is about $0.35 \text{ cm}^3/\text{s}$ (at 298 K).

Compared to this the characteristic flame height was about 10 mm. It is noted that measurements were not conducted at the distances of less than 1 mm from the pine needle surface, due to strong flame perturbations induced by the probe. These perturbations in some of the tests essentially resulted in reduction of the flame spread velocity or even flame extinction as the flame passed by the probe. This is both due to heat loss from the

Table 1. Species and corresponding peaks in the mass spectrum and the relative error (%) of measuring species concentration in the flame of a pine needle.

Species	H_2O	CO	N_2	O_2	CO_2	C_2H_5OH (ethanol)	CH_3COCH_3 (acetone)
Measured mass peak, m/e	18	28	14	32	44	31	43
Error, %	~ 8	~ 5	~ 7	~ 5	~ 5	~ 10	~ 10

flame to the probe (Malhotra and Kumar, 2012) and removal of the combustible pyrolysis products of the pine needles from the flame zone. It was experimentally found that, with the distance from the microprobe to the pine needle surface being 0.2–0.4 mm, the flame extinguishes as it approaches the microprobe. At the distance from the microprobe to the pine needle surface >0.7–1.0 mm, such an effect is absent, indicating that at the distances >1 mm, the microprobe disturbs the flame to a lesser degree.

Calibration of the concentration of the measured species was conducted using gas mixtures of known composition, namely, $N_2 + O_2$, $CO_2 + N_2$, $Ar + CO$, $C_2H_5OH + N_2 + O_2$, $CH_3OCH_3 + N_2 + O_2$, and $H_2O + N_2 + O_2$. The partial pressure of a component in the sample P_i was found by the formula:

$$P_i = K_i \cdot (I_i - I_i^{fon})$$

where I_i and I_i^{fon} are the peak intensities of the i th species in the mass spectrum of the analyzed sample and in the background mass spectrum. K_i is the sensitivity coefficient by the i th species, determined as $K_i = \Delta P_i / \Delta I_i$ in the calibration mixtures. The values of the sensitivity coefficients for the species measured in the pine needle flame are shown in Table 2.

Concentration of the gaseous species in flame expressed in mole fractions was calculated as the ratio of the partial pressure of the measured component P_i to the sum of partial pressures of all the measured components of a gas mixture by the formula:

$$C_i = \frac{P_i}{\sum_j P_j}$$

Measuring temperature in the gas and condensed phases for a burning pine needle

In order to obtain more reliable experimental data on the distribution of the gas temperature in the pine needle flame, we used two independent methods using thermocouples and a pneumatic probe. The thermocouple method is more accurate, as it is a direct method of temperature measurement and disturbs flame to an insignificant degree. The pneumatic probe method is more complicated and sophisticated, and it may implicate significant flame disturbances by a probe. Serious attention is always paid to the important issue of probe-induced flame disturbance. Therefore, comparing the results of measuring the temperature profiles by these two methods allows substantiation validity of the methodology of measuring species concentration with a microprobe in terms of flame

Table 2. Sensitivity factors for the species measured in flame.

Species	K_i
H_2O	$1.5 \cdot 10^{-6}$
CO	$1.2 \cdot 10^{-6}$
N_2	$1.1 \cdot 10^{-6}$
O_2	$9.7 \cdot 10^{-7}$
CO_2	$7.5 \cdot 10^{-7}$
EtOH	$1.7 \cdot 10^{-6}$
C_3H_6O	$1.4 \cdot 10^{-6}$

disturbance, as the species concentration profiles and the temperature profiles are simultaneously measured in the flame by a probe.

Micro thermocouple measurements

Thin Pt–Pt + 10% Rh thermocouples were used to measure the temperature distribution in gas and condensed phase for a burning single vertical pine needle in downward spread configuration. One of the thermocouples (T1) was placed inside the needle. The thermocouple (0.05 mm in diameter) was drawn inside the needle using hard 0.05-mm tungsten wire. The thermocouple junction was placed in the center of the needle (lengthwise as well as at the center of the cross section). The pine needle was fastened vertically by the leads of thermocouple T1. The gas-phase temperature was measured with a 0.02-mm

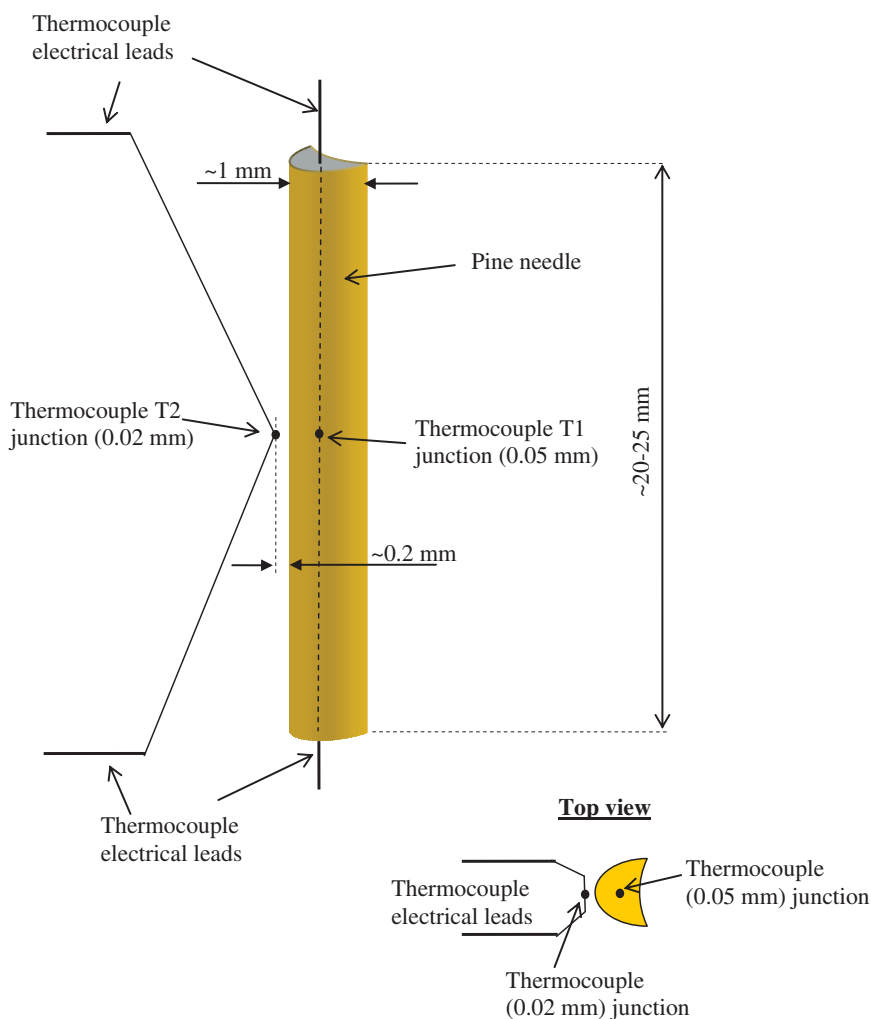


Figure 1. Schematic of a single pine needle fuel sample. Also shown in the figure are thermocouple position for temperature measurements in flame and pine needle.

thermocouple (T2), the junction of which was placed near the mid length of the pine needle. The distance of the thermocouple junction T2 from the surface of the pine needle was set from 0.2 mm to 7 mm. A schematic showing pine needle geometry and relative positions of thermocouples is shown in Figure 1.

The variation of temperature with time was recorded using a multi-channel transducer apparatus E14-140-M (“L-Card”), which ensured measurement of the voltage of direct current in three measurement channels using a 14-bit analog-to-digital converter (ADC) and multi-channel input selector. Two control channels of the converter were used to record the temperature, and the third one was used to synchronize temperature measurement with the video recorder. The E14-140-M apparatus was connected to a PC via a standard USB interface for measurement control and power supply to the apparatus. The temperature was measured at a frequency of 1 kHz and with an accuracy of ± 5 K.

The pine needle was ignited from its top end with a miniature cotton torch wetted with a small amount of ethanol. The process of flame spread along the pine needle was recorded with a digital video recorder. Based on the video results, the pine needle’s flame spread velocity was obtained. The relative accuracy of measurement of flame spread over a pine needle is about $\pm 15\%$, therefore, the accuracy of determining the distance from the flame front to the measurement point is also equal to this value. The temperature distribution along the length of the pine needle was obtained from the flame temperature versus time data and the measured flame spread rate.

To synchronize the temperature measurements with the video recording of the downward burning of the pine needle, a light-emitting diode (LED) was placed in the view of the video recording camera. The LED was connected to the third channel of ADC. During combustion of the pine needle, the LED was turned on using a switch, and this moment was recorded simultaneously in the video recording and the temperature versus time diagrams.

Measuring the temperature distribution in the pine needle’s flame by the pneumatic probe method

The temperature distribution in the gas phase was also measured by a pneumatic probe. The mass flow through a pneumatic probe with the cross section S , with the pressure p_0 and the temperature T_0 , was determined by the ratio (Shapiro, 1953):

$$w = Sp_0 \left(\frac{\gamma M}{RT_0} \right)^{\frac{1}{2}} \left(\frac{2}{\gamma + 1} \right)^b$$

where $b = \frac{\gamma+1}{2(\gamma-1)}$; $\gamma = \frac{c_p}{c_v}$; M is the molecular weight of the gas; c_p , c_v are the isobar and isochoric specific heat capacities of gas; and R is the universal gas constant.

If under experimental conditions the mean molecular weight of gas and its specific heat capacity vary slightly, an expression may be derived that determines dependence of the mass flow of gas through the probe on the gas temperature:

$$\left(\frac{w_1}{w_2} \right)^2 = a \frac{T_2}{T_1}$$

where w_1 and w_2 are the mass flow of the gas at the temperatures T_1 and T_2 , respectively, and a is the coefficient close to 1. The results of the tests conducted show that the maximum change of the mean molecular weight of the combustion products in the pine needle flame over a range of distance of 1–7 mm from the needle surface is not more than 7%. This is because N_2 constitutes the major fraction (~75–79%) of the combustion products.

When gas flows through the probe into the vacuum chamber, the change in the mass flow of gas is proportional with the change in the pressure in the ion source chamber of the mass spectrometer and may be measured by the change in the respective mass peak intensities in the mass spectrum of the sample taken, i.e., $\Delta w_i \propto \Delta P_i \propto \Delta I_i$. Thus, it is possible to quantify not only the composition of a sample but also the temperature of the gas sampled with the probe in one test with a mass spectrometer:

$$T = T_0 \cdot A \cdot \left(\frac{\sum_i P_i^{T_0}}{\sum_i P_i} \right)^2$$

where P_i and $P_i^{T_0}$ are partial pressures of species in the probed sample at the temperatures T and T_0 , respectively. A is the calibration factor. The partial pressures of the components in sample P_i are found by the formula:

$$P_i = K_i \cdot (I_i - I_i^{fon})$$

where I_i and I_i^{fon} are peak intensities of the i th species in the mass spectrum of the sample analyzed and in the background mass spectrum; K_i is the sensitivity factor for the i th species, determined as $K_i = \Delta P_i / \Delta I_i$ in calibration. For determining the unknown temperature of the sample, the initial condition is required; it is convenient to use the composition of gas corresponding to that of air at $T_0 = 298$ K in the given formula.

Error estimation at measurement of pine needle temperature

The temperature measurement error for a thermocouple embedded into a pine needle is related to heat exchange between the thermocouple and the environment, as well as to the heat loss to its cold leads. To evaluate this error, the following differential equation describing the temperature profile in the thermocouple embedded inside a pine needle was used. The equation was arrived at by considering heat exchange between the thermocouple and the environment:

$$0 = \lambda_1 \frac{d^2 T_1}{dz^2} - \alpha_1 ((T_1 - T_e)) r_1^{-1}$$

where λ_1 is thermal conductivity for the thermocouple (λ_1 for platinum equals to 1 W/(m·K)); T_1 is the temperature measured by the thermocouple; r_1 is the radius of the thermocouple's junction (15×10^{-6} m); α_1 is the coefficient of heat-exchange between the thermocouple and air (α_1 equals to 150 W/(K·m²); and $T_e(x)$ is temperature profile in the

pine needle. The thermocouple is in contact with the pine needle and the gas in the pine needle's pores. It was assumed that the most heat transfer to the thermocouple occurred with gas in the pine needle pores. The temperature profile measured by the thermocouple was described by the function shown in Figure 2. Numerical coefficients in the function were selected to best match the experimental data. To calculate the numerical coefficients in the equation in Figure 2, a software package for scientific graphing and data analysis, Sigma Plot 8.0 (<http://www.sigmaplot.com>), was used. The temperature measurement error was calculated using the above equation. The maximum error was estimated to be about 3×10^{-6} K. The estimated time response for the 20-micron and 50-micron bead diameter thermocouples were 1.67×10^{-6} s and 1.1×10^{-5} s, respectively.

The measurement of downward flame spread velocity along a vertically positioned pine needle in air counter-flow

To measure the downward flame spread velocity along a vertical pine needle for various counter-flow air velocity, a vertical wind tunnel type facility was used. Figure 3 shows the schematic of the setup and configuration of the pine needle. The pine needle was placed in a tubular test section and its position was secured at the lower end in a wire holder. The tubular test section was preceded by a convergent conical section to even the velocity of the air flow in the narrow part of the tubular test section. Ahead of the convergent section in the lower wider part of the tube porous diaphragms were placed to make air velocity in the tube uniform. The air flow was supplied to the lower part of the tube through a mass flow regulator with accuracy not lower than $\pm 1\%$. The air flow velocity in the test section was varied over the range of 0 to 13.2 cm/s and was determined by the value of the volume air flow rate and the cross section area of the narrow part of the tube.

First two marks were made on the pine needle. The first mark was at 7–10 mm from the top end of the pine needle and the second was at the distance of 30 mm from the first. The pine needle was secured in position by a holder ignited from above and air flow was supplied. The time elapsed for the passage of flame front between the marks on the pine

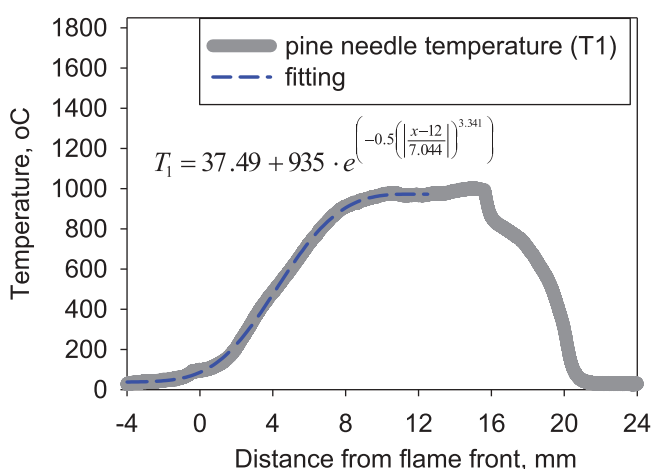


Figure 2. A typical measured temperature profile in the pine needle and described by function T_1 .

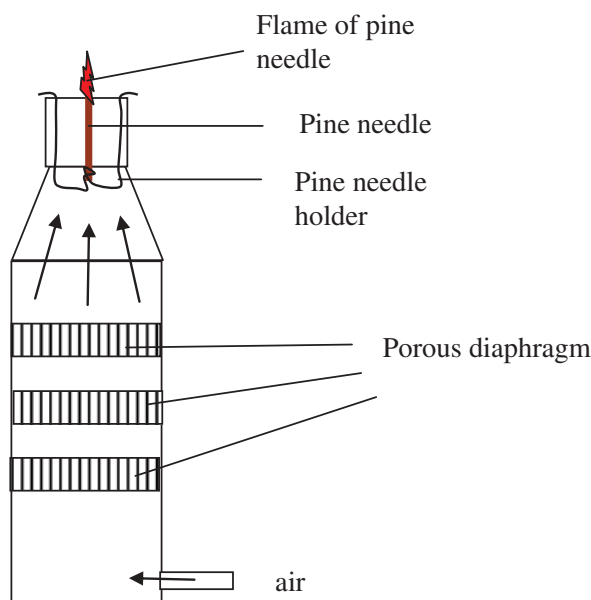


Figure 3. A schematic of apparatus used for determining the downward flame spread rate of a single pine needle in counter-flow of air flow.

needle was measured. The burning velocity was determined by dividing distance traversed by the flame front (30 mm) by the elapsed time. Our preliminary experiments showed that the steady flame spread rate over a pine needle becomes established rather fast, approximately within 2–3 s after the pine needle gets ignited (which corresponds to 3–4 mm shifting of the flame front from the pine needle's end). The measurements were made after the flame spread rate became steady. The maximum variation of the flame spread rate value in still air for different pine needle samples was about $\pm 15\%$ of the mean value determined in 10 tests. The tests were conducted 5–10 times for each value of the air flow velocity. The mean flame spread velocity was calculated and the measurement errors were evaluated from the data set obtained from these tests.

Results and discussion

The thermal structure of the pine needle flame

The variation of the flame temperature along the length of a pine needle was measured with a micro thermocouple and a pneumatic probe at various fixed distances away from the surface of the pine needle. This distance perpendicular to the length of pine needle varied from 1 mm to 7 mm. The experimental results shown in Figures 4–9 were obtained in still air. The measured temperature data are plotted for various distances from the pine needle surface (1–7 mm in steps of 1 mm) and shown in Figures 4a–4g. The position of 0 mm in the plots corresponds to the position of the flame front. The position of the flame front ($x = 0$ mm) corresponds to the moment of the visible flame edge (the blue zone) reaching the location on the pine needle surface of the junction of the thermocouple

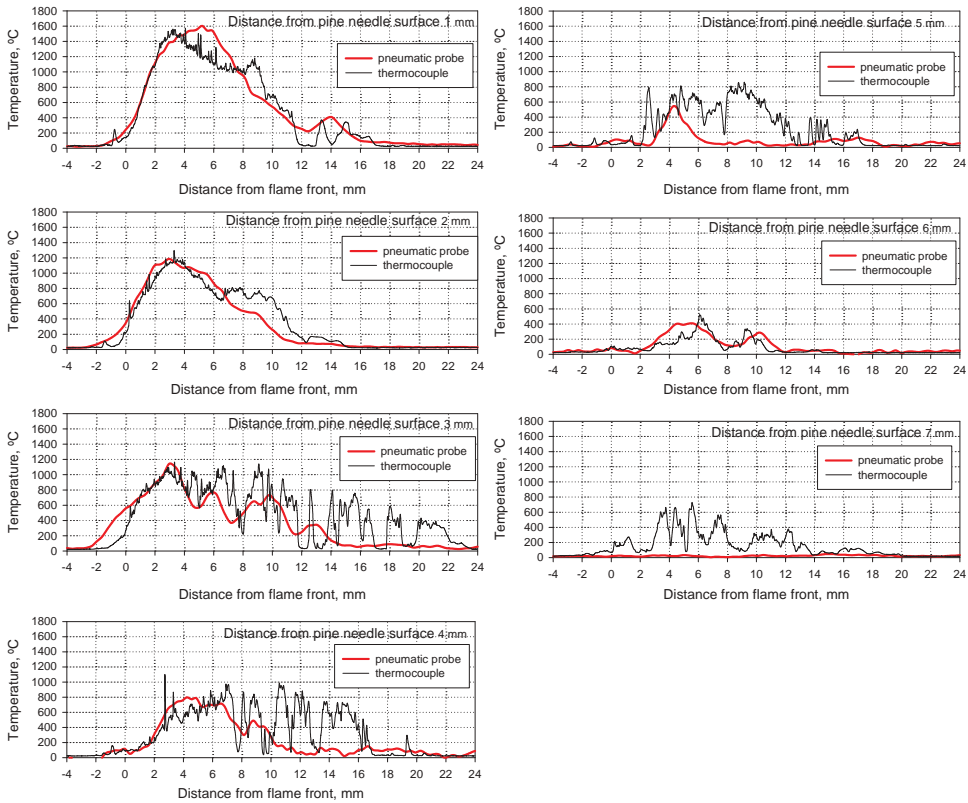


Figure 4. Temperature profiles in gas phase at various fixed distances perpendicular to the pine needle surface (1 mm, 2 mm, 3 mm, 4 mm, 5 mm, 6 mm, 7 mm). The temperatures are measured by micro-thermocouple and pneumatic probe for downward spreading flame along pine needle.

embedded into the pine needle. This place is opposite the microprobe or the thermocouple located in the gas phase. It is noted that the measured temperature data with the two methods agree satisfactorily for the maximum temperature in the flame. However, micro thermocouple measurements indicate that the extent of the heated zone (in the direction perpendicular to the surface of the pine needle) is greater than that measured with the pneumatic probe. In the pneumatic probe method essential averaging of the temperature across a local finite volume occurs. Therefore, the temperature profiles obtained by this method are “smoother,” and the heated zone turns out to be smaller. The micro-thermocouple measurements are more sparsely localized, which can be seen in the significant “noise” present in the temperature profiles. These temperature fluctuations are caused by flame fluctuations related to variations in the evolving of pyrolysis products (gas micro jets) from the pine needle surface, which were recorded in the video of the burning process.

Based on the matrix of data obtained, the temperature profiles in a direction perpendicular to the pine needle was determined at different positions (2.3 mm, 6.3 mm, 8.2 mm, and 12 mm) from the pine needle’s flame front ($x = 0$). The temperature profiles in the direction perpendicular to the pine needle were obtained from the temperature profiles measured along the pine needle at the distances of 1–7 mm from its surface. Thus, the temperature profiles along the pine

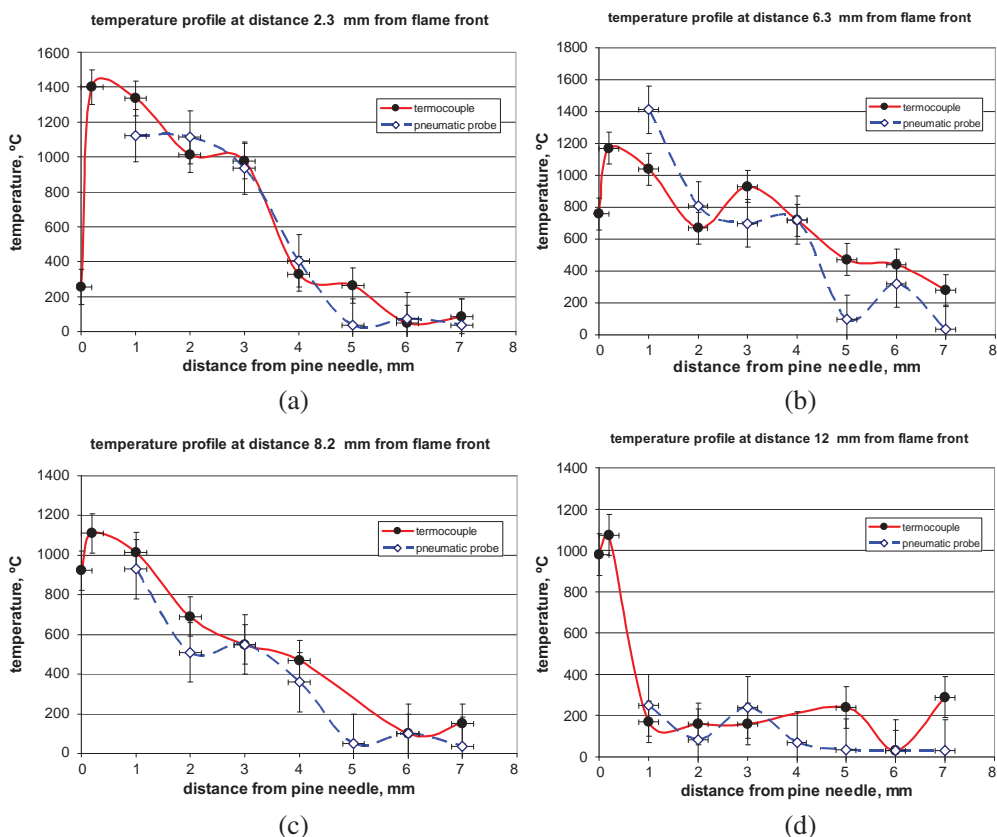


Figure 5. Temperature profiles in the flame of a pine needle in the direction perpendicular to the pine surface at the distance of (a) 2.3 mm, (b) 6.3 mm, (c) 8.2 mm, and (d) 12 mm from the flame front ($x = 0$).

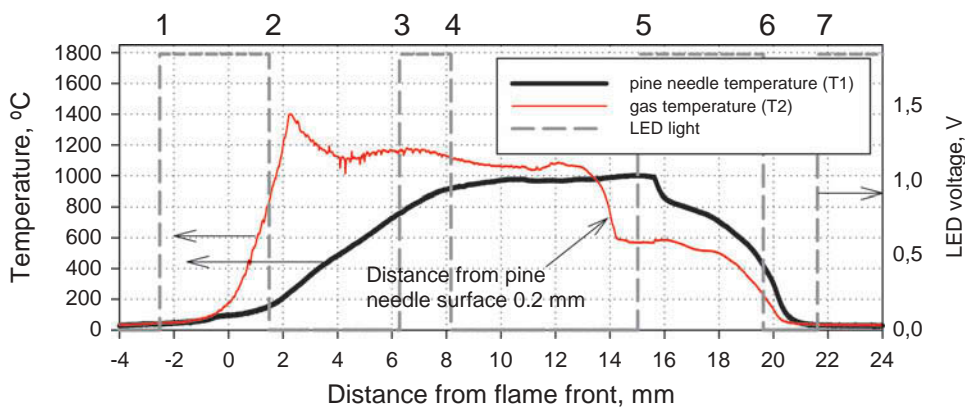


Figure 6. Temperature profiles in gas phase at 0.2 mm perpendicular to the pine needle surface and condensed phase (center of pine needle) for a downward spreading flame over a single pine needle.

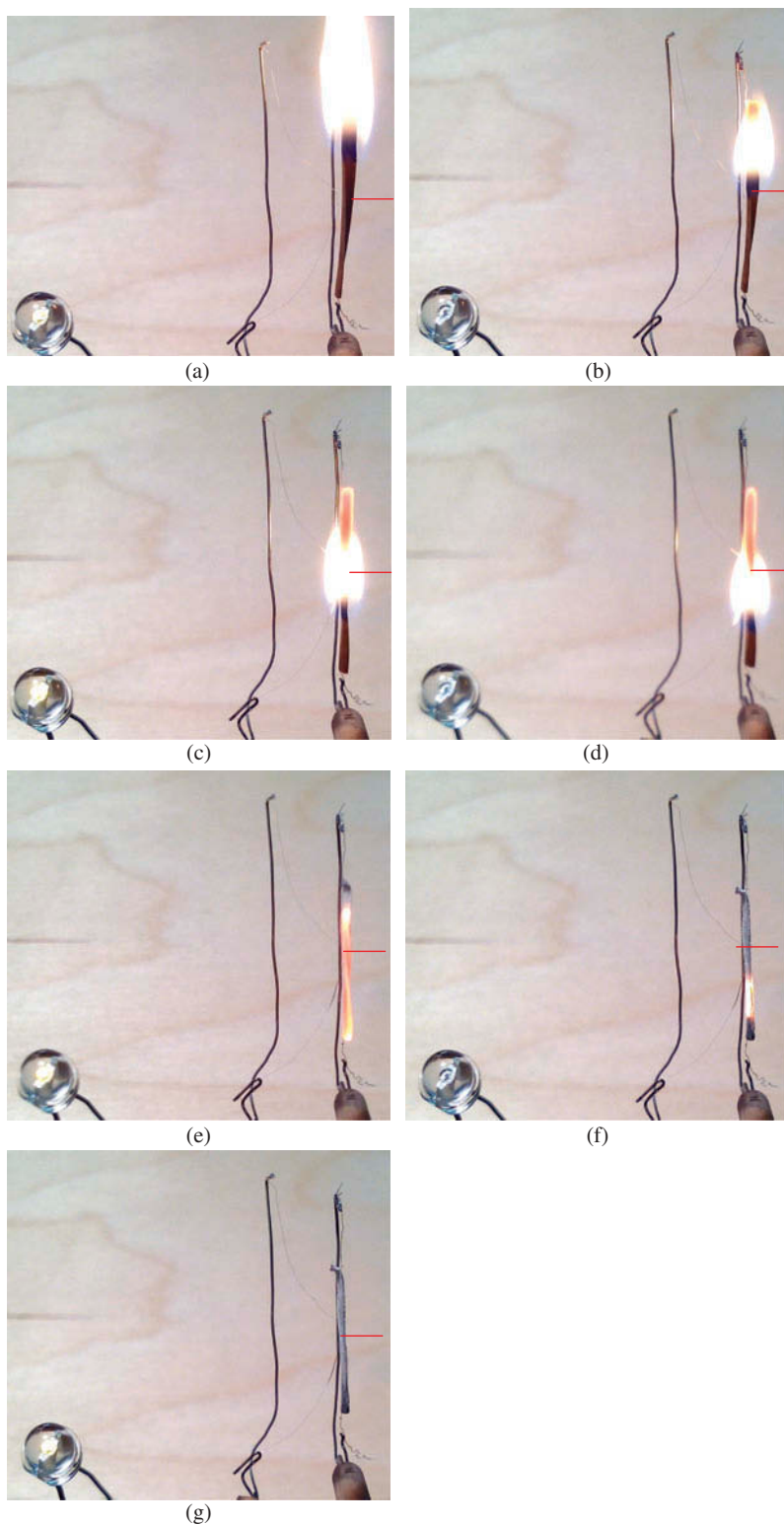


Figure 7. Instantaneous pictures of downward flame spread over a single pine needle of length 20 mm. These various instants during the flame spread process are indicated in [Figure 6 \(1–7\)](#).

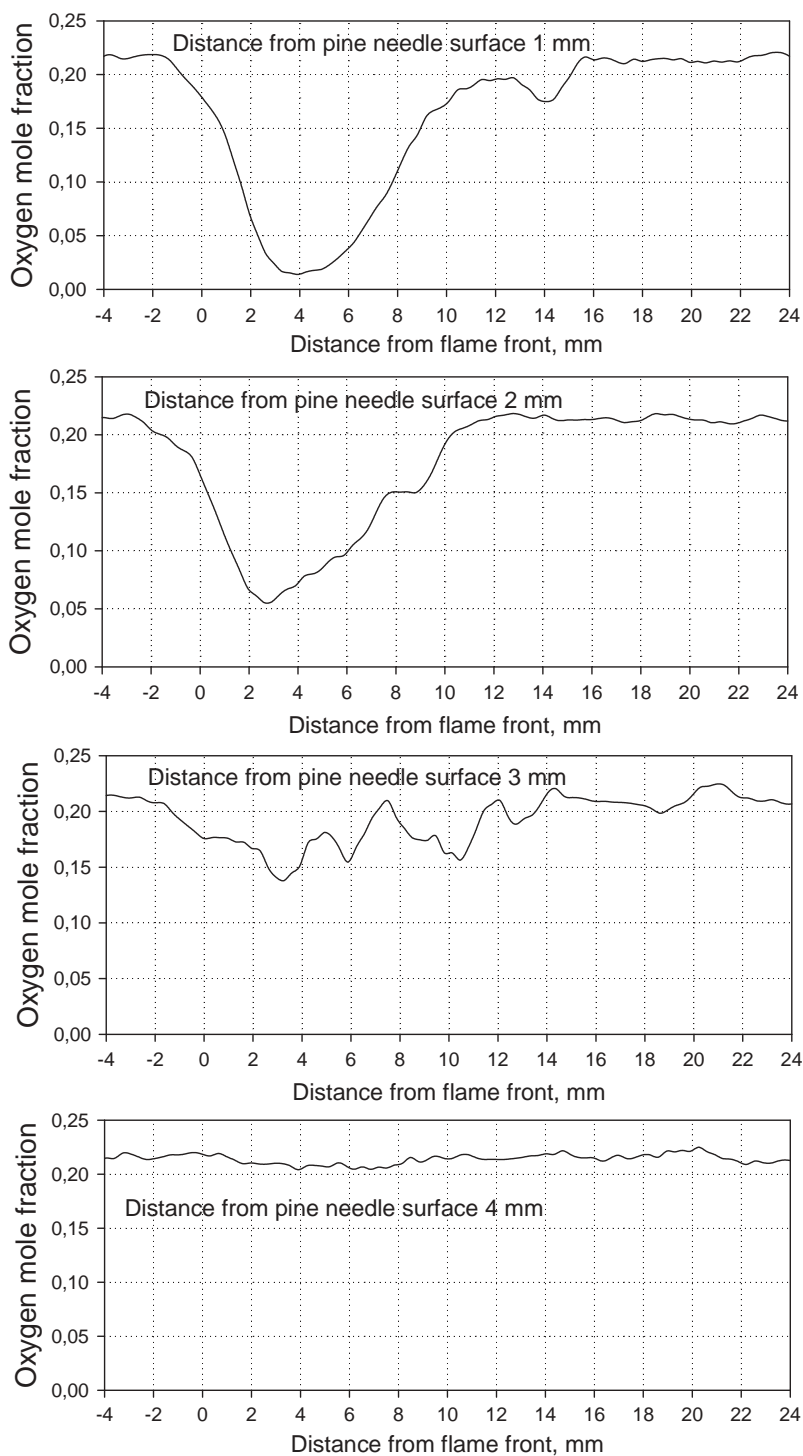


Figure 8. Measured profiles of O_2 concentration in mole fraction in the downward spreading flame over a pine needle. The temperatures are plotted at various fixed distances perpendicular to the pine needle surface (1 mm, 2 mm, 3 mm, and 4 mm).

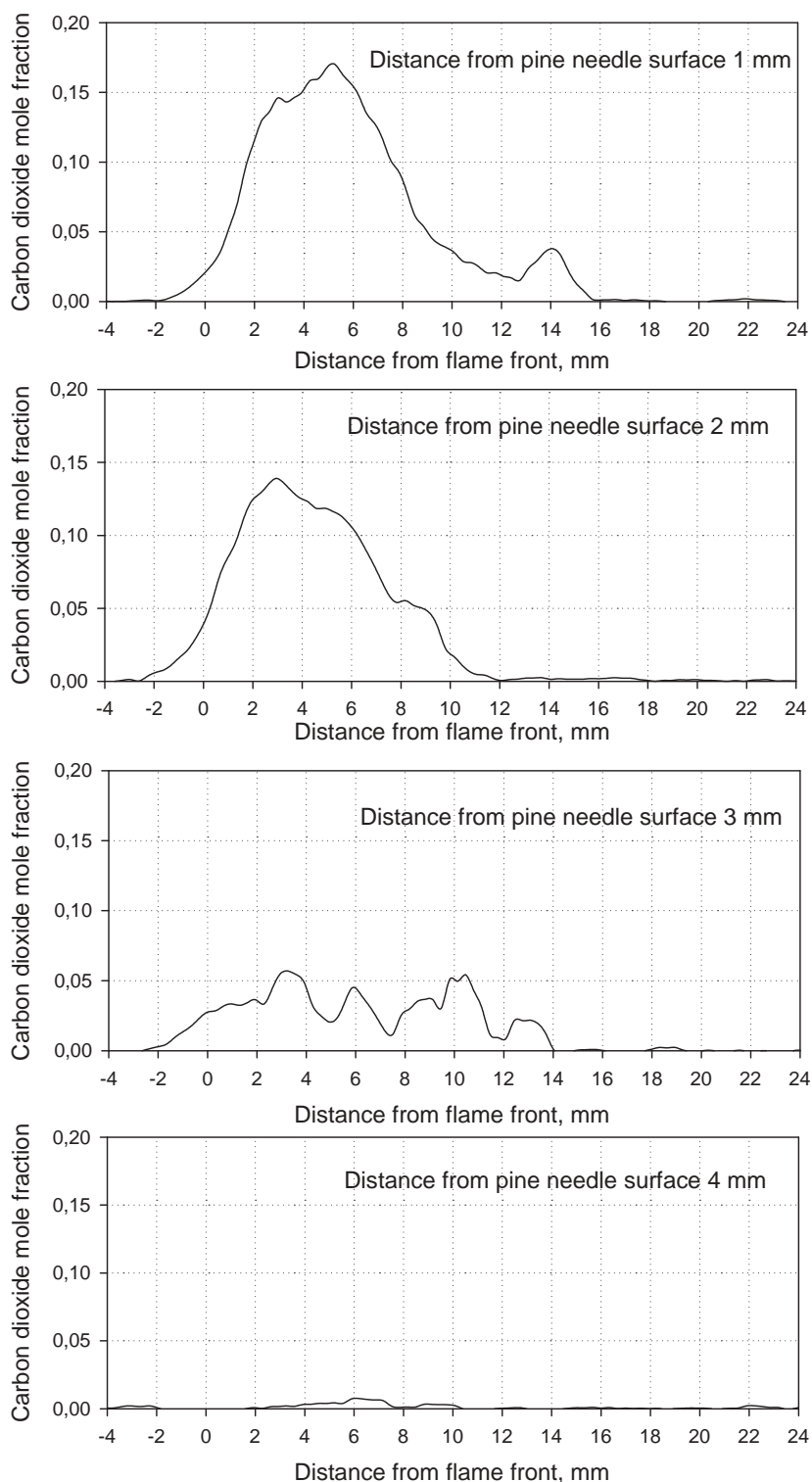


Figure 9. Measured profiles of CO₂ concentration in mole fraction in the downward spreading flame over a pine needle. The temperatures are plotted at various fixed distances perpendicular to the pine needle surface (1 mm, 2 mm, 3 mm, and 4 mm).

needle were measured in one experiment, and the temperature profiles in the direction perpendicular to the pine needle were measured in a series of experiments. These temperature data for both micro thermocouple and pneumatic probe are shown in Figures 5a–5d. In addition to temperature measurements at the distances of 1–7 mm from the pine needle's surface (shown in Figure 4), the temperature profiles in the pine needle (T1) and temperature near its surface at the distance of 0.2 mm (T2) were also measured. In all of the subfigures of Figure 5 the temperature is seen to rise from surface to maximum at distance between 0.2 mm and 1 mm perpendicular to the fuel surface and decrease with further increase in this distance. We attribute the appearance of “wiggles” in the temperature profiles in Figure 5 to several factors. The first factor is local fluctuations in the gas fluxes evolving from the pine needle surface. That was established from the video of the pine needle burning. The other factor is the differences among the pine needle samples, as the profiles shown in Figure 5 are the result of several experiments. The flame half width (extent perpendicular to pine surface) is about 6–7 mm and is seen to shrink to about 1 mm at 12 mm downstream of the flame front. Thus, the flame length is about 12 mm. Figure 6 further shows the temperature profiles measured in the pine needle (T1) and in the flame (T2) at the distance from the pine needle surface of 0.2 mm for the downward spreading flame. It is interesting to note that the pine surface temperature exceeds gas phase temperature for distances greater than 13.5 mm measured from the flame front ($x = 0$). This suggests that char oxidation is taking place, which increases temperature of the pine needle surface after passage of the flame. Figure 6 also shows variation of the voltage at the LED leads with time. This allowed identification of different moments of time in the video record of the flame propagation process. Figures 7a–7g show images of flame extracted from video at seven instances marked in Figure 6. In these figures, a horizontal line indicates the position of the junctions of thermocouples T1 and T2.

One can note that, as flame spreads down the pine needle, the measured flame temperature (at distance 0.2 mm from pine surface) increases much more rapidly than the temperature inside the pine needle (see Figure 6). At the instant of time shown in Figure 7b, the temperature in the gas phase is 860°C, while the temperature of the pine needle is only 160°C (see Figure 6). This position corresponds to a distance of 1.5 mm downstream of the flame front ($x = 0$). At the distance of 2.3 mm downstream of the flame front, the flame temperature grows to the maximum value of 1400°C, whereas the temperature of the pine needle increases to 250–300°C. The temperature profiles in this zone in the direction perpendicular to the pine needle are shown in Figure 5a. One can suppose that the maximum flame temperature corresponds to the flame zone in which the rate of pyrolysis with volatile products formed and their flux from the pine needle surface are maximal. In this zone, concentrations of CO₂ and H₂O at the distance of 1 mm from the pine needle surface are also maximal (discussed in the section below). Figure 7c corresponds to the position of thermocouple T2 at the distance of 6.3 mm from the flame front. As the flame passes through this zone, the flame temperature decreases to 1160°C, while the temperature of the pine needle grows to 770°C. In this zone, the rate of reaction leads to formation of volatile pyrolysis products and their flux decreases due to consumption of the fuel, despite the growth of the pine needle's temperature. The flame temperature profiles in this zone in perpendicular to the pine needle are shown in Figure 5b. At such temperatures (of about 770°C), the pyrolysis processes are practically over, which can be noted in the subsequent reduction of the flame temperature in the gas phase to 1130°C, as well as in the increase of the temperature inside the pine needle to

920°C (Figure 7d). This location in Figure 6 corresponds to the distance from the flame front equal to 8.2 mm. The flame temperature profile in this zone in the direction perpendicular to the pine needle is shown in Figure 5c. After propagation of brightly glowing flame along the pine needle, the stage of char burning is observed by the bright orange glowing of the char (Figures 7c and 7d). As char burns, the temperature of pine needle grows from 920°C to 1000°C. This is supposed to be related to reduction in the heat loss due to radiation, as a layer of ash is formed, which has lower emissivity compared to char. The flame temperature profile in this zone in a direction perpendicular to the pine needle is shown in Figure 5d. As soon as the glowing flame reaches the lower end of the pine needle and is extinguished, the temperature in the gas phase drops to 560–580°C, whereas the temperature in the char still remains high for some time—about 1000°C (Figure 7e). Finally, char combustion stops at a small section near the lower end of the pine needle (Figure 7f). At that, the temperature both in the gas phase and in the condensed phase decreases rapidly to room temperature (Figure 7g).

The chemical structure of pine needle flame

The pneumatic micro-probe data for concentration of O₂, CO₂, and H₂O measured in the gas phase at various distances away from the pine needle surface over a period of flame propagation was converted into spatial data with respect to flame front by use of flame spread rate. These data for O₂, CO₂, and H₂O concentration varying with distance to the flame front measured at different distances from the pine needle surface are shown in Figures 8–10 in the respective order. In Figure 8, it is seen that the minimum concentration of O₂ in the flame near the surface of the pine needle (at the distance of 1 mm away from it) is about 1.5%, while concentration of CO₂ and H₂O are 16% (Figure 9) and 10% (Figure 10), respectively. This is noted to occur at 3–5 mm downstream of the flame front. Thus, within the limits of the measurement accuracy, at the distance 1 mm from the pine needle, practically all of the oxygen in the air turns into combustion products. Synchronization of the position of the probe in relation to the flame front for the profiles of species concentrations measured along the axis of the pine needle at a fixed distance from it allowed the distribution of species concentrations in the plane perpendicular to the axis of the pine needle to be obtained. The profiles of O₂, CO₂, and H₂O concentration in the direction perpendicular to the pine needle's surface at the distance of 2.3 mm and 3.5 mm from the flame front are shown in Figure 11. Extrapolating the obtained dependence of O₂ concentration to the pine needle surface, we can see its concentration on the pine needle surface is practically equal to zero at these locations.

The pyrolysis process of the pine needle takes place in two stages: (1) pyrolysis of the pine needle with volatile products and char formed; and (2) oxidation of char with air oxygen with oxidation products CO, CO₂, and H₂O formed. Therefore, two combustion zones may be identified in the direction of flame propagation down the pine needle: (1) the zone of the pine needle's burning with char and volatile pyrolysis products formed, followed by combustion of the latter; and (2) heterogeneous burning of char.

Based on the measured concentration results, N₂ concentration in flame at the distance of more than 1 mm from the surface of the pine needle is practically constant within the accuracy limits of the measurements. This suggests that the flow velocity of the gaseous pyrolysis products of the pine needle from its surface is low enough, so they practically do

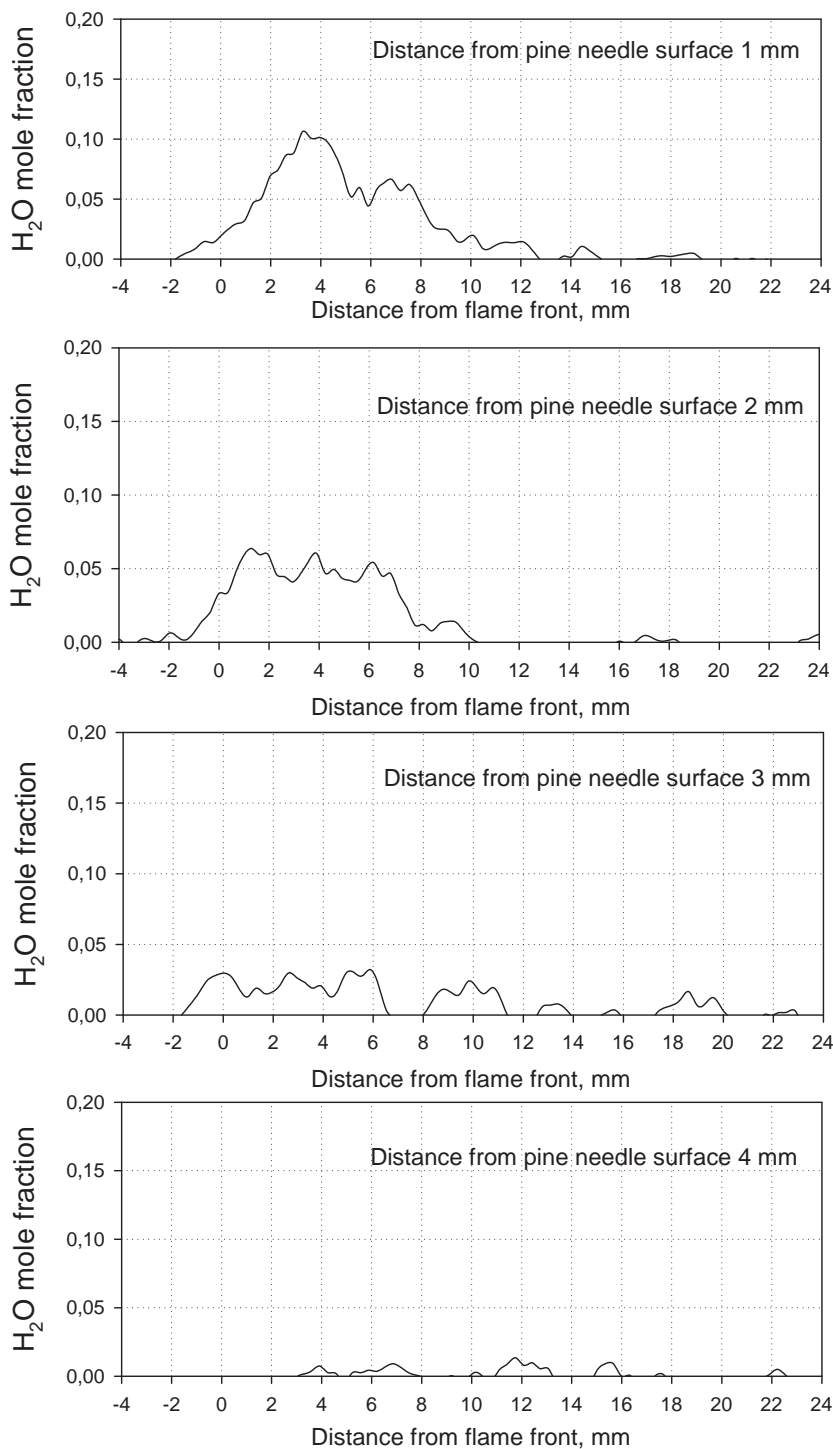


Figure 10. Measured profiles of H₂O concentration in mole fraction in the downward spreading flame over a pine needle. The temperatures are plotted at various fixed distances perpendicular to the pine needle surface (1 mm, 2 mm, 3 mm, and 4 mm).

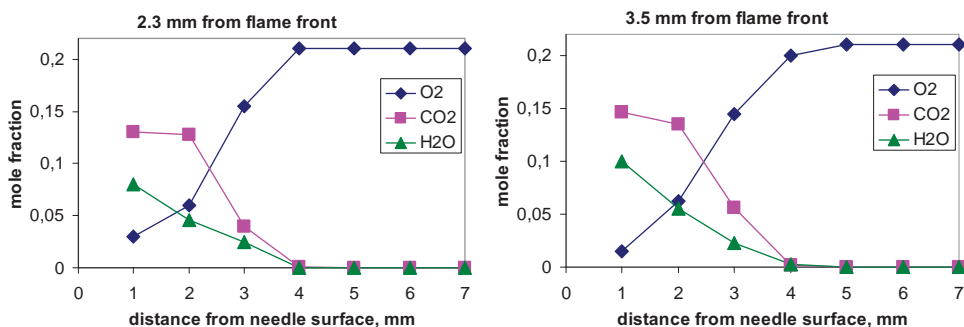


Figure 11. Concentration profiles of O₂, CO₂, and H₂O in the flame of a pine needle in direction perpendicular to the pine needle surface and at a distance of (a) 2.3 mm and (b) 3.5 mm from the flame front ($x = 0$).

not substitute the inert diluent from the combustion zone. This is also confirmed from the measurements of the concentrations of C₂H₅OH and CH₃OCH₃, from which it follows that measurable concentration of these species are observed only near the surface of the pine needle and is only about 0.3–0.5%. Thus, the consumption zone of the given pyrolysis products is rather narrow, about 1–2 mm wide near the surface of the pine needle. As shown above, at this distance maximum flame temperature is achieved; therefore, we can assume that the major heat production occurs in a region 1 mm or 1.5 mm wide near the surface of the pine needle.

Flame spread velocity at downward flame propagation along a single pine needle at counter-flow of air

Finally the dependence of the downward flame spread rate along a pine needle on the opposed air flow velocity was studied. Figure 12 shows the variation of downward flame spread velocity with opposed flow velocity. As can be seen from the figure, the flame

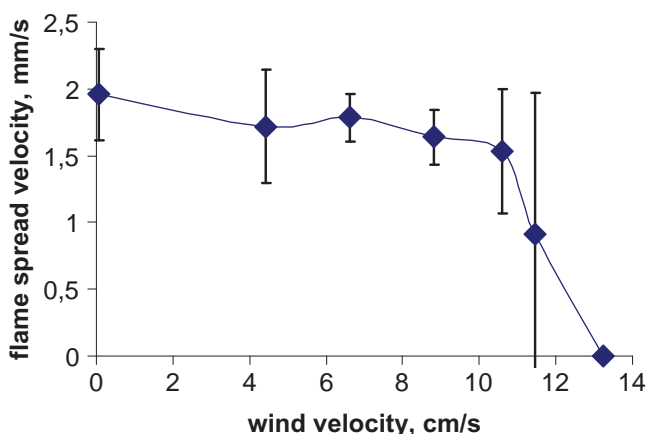


Figure 12. Variation of downward flame spread rate over a vertical pine needle with counter-flow of air velocity.

spread rate at '0' air velocity was about 2 mm/s. With the increase in air flow velocity from 0 to 11.5 cm/s, the flame spread rate decreases by about 20%. As the air flow velocity is increased further, the flame spread velocity decreases steeply, and when the air flow velocity exceeds 13 cm/s, the flame does not spread.

Conclusion

In this work a detailed experimental study on downward flame spread over single vertically placed pine needles of *Pinus Sibirica* was carried out. Based on the present study, the following salient features and conclusions may be drawn:

- (1) The complete temperature field in the gas phase and the temperature profile in the condensed phase were measured by the micro thermocouple technique for downward flame propagation along a single pine needle. The temperature field in the gas phase was also obtained using an alternate pneumatic micro-probe technique and the two techniques gave a consistent temperature field data.
- (2) The concentration profiles of O_2 , the main combustion products (CO_2 , CO , H_2O) and of the volatile pyrolysis products were measured using the method of mass-spectrometric micro probe sampling from the downward spreading flame along a single pine needle. Thus, a detailed chemical structure of the flame was obtained.
- (3) Dependence of the flame spread velocity on the counter-flow rate of air was measured for downward flame propagation along a single pine needle. Within the range of the air flow rate varying from 0 to 10 cm/s, the flame spread velocity decreased slightly (by 10%), while in the range from 10 cm/s to 13 cm/s, it dropped considerably up to complete extinction.
- (4) The measured data on temperature and species clearly reveal two stages of pine needle combustion. In the first stage, formation of char and volatiles subsequently combust in the gas phase to form a propagating flame; in the second stage, char oxidizes to form ash. The experimental data also shows separation of these two stages, as immediate downstream of the flame front there is a region devoid of any oxygen.
- (5) The detailed temperature and concentration data along with flame spread measurements at various opposed flow velocities constitute a useful set of data for development and validation of a numerical model of downward flame propagation over charring fuels (in this case, along a single pine needle). The data obtained and the applied methods of research would be of interest to those studying the polymer combustion mechanism.

Funding

This work was supported by the RSF and DST under Grant No. 16-49-02017.

References

Albini, F.A. 1981. A model for the wind-blown flame from a line fire. *Combust. Flame*, **43**, 155–174.

- Bhattacharjee, S., and Altenkirch, R.A. 1992. A comparison of theoretical and experimental results in flame spread over thin condensed fuels in a quiescent, microgravity environment. *Proc. Combust. Inst.*, **24**, 1669–1676.
- Brunauer, S., Emmett, P.H., and Teller, E. 1938. Adsorption of gases in multimolecular layers. *J. Am. Chem. Soc.*, **60**, 309–319.
- Fernandez-Pello, A.C., and Williams, F.A. 1975. Laminar flame spread over PMMA surface. *Proc. Combust. Inst.*, **15**, 217–231.
- Hsu, S.-Y., and T'ien, J.S. 2011. Flame spread over solids in bouyant and forced concurrent flows: Model computations and comparison with experiments. *Proc. Combust. Inst.*, **33**, 2433–2440.
- Konev, E.V. 1977. *Physical Foundations of the Combustion of Vegetable Materials*, Novosibirsk, Nauka, Russia.
- Konev, E.V., and Sukhinin, A.I. 1977. The analysis of flame spread through forest fuel. *Combust. Flame*, **28**, 217–223.
- Korobeinichev, O.P., Tereshchenko, A.G., Paletsky, A.A., Gonchikzhapov, M.B., Shundrina, I.K., Kataeva, L.Yu., Maslennikov, D.A., Naganovsky, Y.K., and Liu, N. 2014. Kinetics of pine needles pyrolysis. Presented at the 8th International Seminar on Flame Structure, Berlin, Germany, September 21–24. Available at: <http://flame-structure-2014.com/wp-content/uploads/Paletsky-Alexander.pdf>
- Kumar, C., and Kumar, A. 2012. On the role of radiation and dimensionality in predicting flow opposed flame spread over thin fuels. *Combust. Theor. Model.*, **16**, 537–569.
- Kumar, K.M.N., and Kumar, A. 2017. The dynamics of near limit self-propagating flame over thin solid fuels in microgravity. *Proc. Combust. Inst.*, **36**, 3081–3087.
- Lyons, P.R.A., and Weber, R.O. 1993. Geometrical effects on flame spread for wildland fine fuels. *Combust. Sci. Technol.*, **89**, 153–165.
- Malhotra, V., and Kumar, A. 2012. Effect of gas phase heat sink on suppression of downward flame spread over thin solid fuels. *Int. J. Adv. Eng. Sci. Appl. Math.*, **4**, 138–151.
- Morandini, F., Simeoni, A., Santoni, P.A., and Balbi, J.H. 2005. A model for the spread of fire across a fuel bed incorporating the effects of wind and slope. *Combust. Sci. Technol.*, **177**, 1381–1418.
- Morvan, D. 2013. Numerical study of the effect of fuel moisture content (FMC) upon the propagation of a surface fire on a flat terrain. *Fire Saf. J.*, **58**, 121–131.
- Santoni, P.-A., Marcelli, T., and Leoni, E. 2002. Measurement of fluctuating temperatures in a continuous flame spreading across a fuel bed using a double thermocouple probe. *Combust. Flame*, **131**, 47–58.
- Shapiro, A.H. 1953. *Dynamics and Thermodynamics of Compressible Fluid Flow*, Ronald Press, New York.
- Sibulkin, M., Ketelhut, W., and Feldman, S. 1974. Effect of orientation and external flow velocity on flame spreading over thermally thin paper strips. *Combust. Sci. Technol.*, **9**, 75–77.
- Singh, A.V., and Gollner, M.J. 2015. Estimation of local mass burning rates for steady laminar boundary layer diffusion flames. *Proc. Combust. Inst.*, **35**, 2527–2534.
- Sirignano, W.A. 1972. A critical discussion of theories of flame spread across solid and liquid fuels. *Combust. Sci. Technol.*, **6**, 95–105.
- Sukhinin, A.I. 1975. On temperature distribution I combustion of a bed of pine needles. *Fizika Goreniya i Vzryva.*, **6**, 850–855.
- Weber, R.O. 1990. Modelling fire spread through fuel beds. *Prog. Energy Combust. Sci.*, **17**, 67–82.
- Weber, R.O., and De Mestre, N.J. 1990. Flame spread measurements on single Ponderosa pine needles: Effect of sample orientation and concurrent external flow. *Combust. Sci. Technol.*, **70**, 17–32.
- Wichman, I. 1992. Theory of opposed flow flame spread. *Prog. Energy Combust. Sci.*, **18**, 553–593.